

Adsorption and electronic properties of PTCDA molecules on Si(111)-(7×7): Scanning tunneling microscopy and first-principles calculations

Nicoleta Nicoara,¹ Óscar Paz,¹ Javier Méndez,² Arturo M. Baró,² José M. Soler,¹ and José M. Gómez-Rodríguez¹

¹*Depto. Física de la Materia Condensada, Universidad Autónoma de Madrid, E-28049 Madrid, Spain*

²*Instituto de Ciencia de Materiales de Madrid, CSIC, E-28049 Madrid, Spain*

(Received 19 July 2010; published 4 August 2010)

Scanning tunneling microscopy (STM) experiments and density-functional theory (DFT) calculations are combined to unravel the complex shifts and splittings of molecular orbitals (MOs) for the prototype system of a single π -conjugated molecule bonded to a semiconductor surface. Intramolecular resolution in STM images of 3,4,9,10-perylene tetracarboxylic dianhydride (PTCDA) on Si(111)-(7×7) cannot be understood as resulting from a simple rigid shift of the MOs of the free molecule. DFT calculations and simulations of STM images with realistic tips show large splittings of the original MOs that contribute in a complex way to the tunnel current and are understood under symmetry and charge-transfer arguments. The system is characterized by a strong, partially ionic covalent bonding involving the carboxyl groups of the PTCDA and the Si dangling bonds.

DOI: [10.1103/PhysRevB.82.075402](https://doi.org/10.1103/PhysRevB.82.075402)

PACS number(s): 68.37.Ef, 68.43.Fg, 71.15.Mb, 73.20.Hb

The adsorption and electronic structure of π -conjugated molecules on solid surfaces have been the subject of intensive studies in the last few years both for fundamental and applied reasons.¹ The combination of scanning probe microscopy experiments with first-principles calculations have revealed its power regarding issues as chemisorption, charge transfer, electronic level alignments, molecular-orbital (MO) modifications or electronic transport through single molecules.^{2–10} PTCDA (3,4,9,10-perylene tetracarboxylic dianhydride) has been considered a prototype molecule for these kind of studies on metal surfaces.¹¹ For semiconductors, however, PTCDA has been studied mainly on passivated surfaces as H terminated Si(111),¹² Se or S terminated GaAs(001),¹³ or metal induced reconstructions of Si(111).¹⁴ Although the study of adsorption of other organic molecules on pristine semiconductor surfaces has known also a fast development in the last decade,^{15–20} surprisingly enough there are scarce and early studies dealing with the analysis of adsorption of PTCDA on nonpassivated Si(111)-(7×7) surfaces.²¹

In this work, we present a combined experimental scanning tunneling microscopy (STM) and first-principles calculations analysis of the adsorption and electronic structure of PTCDA on Si(111)-(7×7). The intramolecular resolution observed on experimental images cannot be understood under arguments related to simple energy shifts of the MOs of the free molecules applicable for much less reactive metal surfaces.^{11,22,23} On the contrary, it is shown here that they are the result of more complex splittings and shifts and a complete understanding of the STM images cannot be attained unless first-principles computations of the interacting system as well as STM simulations with realistic tips are performed.

The experiments were carried out in an ultrahigh vacuum system equipped with a homebuilt STM. PTCDA was deposited at room temperature (RT) on clean reconstructed Si(111)-(7×7). Electronic structure calculations and simulated STM images were carried out within density-functional theory (DFT) in the local-density approximation²⁴ using the SIESTA method.^{25,26} The tunneling current between the tip

and the sample was computed with a new efficient method.²⁷ Both, experimental and simulated data were displayed using the WSXM software.²⁸

Figure 1(a) shows a STM image corresponding to the initial stage of adsorption of PTCDA on the Si(111)-(7×7) surface at RT. The adsorbates are imaged as bright protrusions, randomly distributed on the surface. Some of them have similar shape and orientation: they are those adsorbed on the corner hole of the Si(111)-(7×7) reconstruction. On these features, careful STM imaging can lead to intramolecular resolution that depends on the applied bias voltage. Typically, while for large positive voltages the molecule is characterized by two lateral oval-like shapes [Fig. 1(a)], a modified internal structure, consisting of five parallel stripes is imaged when decreasing the voltage [Figs. 1(b) and 1(c)]. This five-stripe pattern is obtained either for low positive voltages or for a wide range of negative voltages. By comparing the distance between the outer stripes and their length with the PTCDA dimensions, it may be inferred that the long axis of the molecule is oriented perpendicular to the stripes and aligned parallel to the dimer line of the (7×7), i.e., the $[01\bar{1}]$ direction. From these experimental findings, simple geometrical considerations indicate that the molecular adsorption of a PTCDA molecule on the corner hole, through bonding with four silicon corner adatoms, might be favored. This is outlined in the schematic (7×7) reconstruction in Fig. 1(d). The distance between the Si adatoms along the $[01\bar{1}]$ direction equals approximately the length of the PTCDA long axis while the separation between the closest two corner adatoms is only slightly larger than the short side of the molecule.

Further information related to PTCDA adsorption can be extracted from STM images. A direct comparison with the MOs of a free PTCDA (Fig. 2) shows that the lowest unoccupied molecular orbital (LUMO)+1 resembles the five-stripe pattern resolved in Fig. 1(b). This finding confirms the previous assumption regarding the PTCDA long axis and its orientation with respect to the substrate, and also suggests a planar adsorption configuration. In terms of electronic struc-

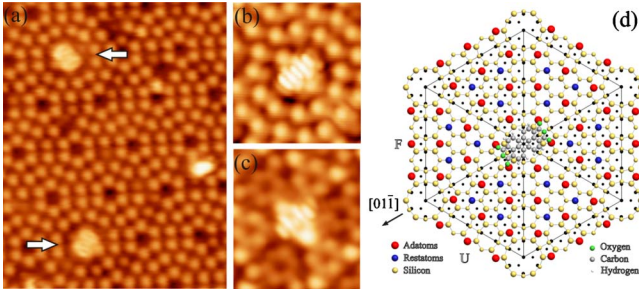


FIG. 1. (Color online) (a) STM image ($11 \times 14 \text{ nm}^2$, $V = +1.5 \text{ V}$, and $I = 0.27 \text{ nA}$) of the Si(111)-(7 \times 7) surface after exposure to PTCDA. The arrows point to single molecules adsorbed on the corner hole site. [(b) and (c)] Intramolecular resolution observed on the same $4.2 \times 4.6 \text{ nm}^2$ area under different conditions: (b) $V = +0.4 \text{ V}$, $I = 0.3 \text{ nA}$ and (c) $V = -1.5 \text{ V}$, $I = 0.26 \text{ nA}$. (d) Schematic view of PTCDA on Si(111)-(7 \times 7).

ture, the observation of the LUMO+1 at energies near and below E_F is unusual. At most, it could be explained by a considerable charge transfer that completely fills the LUMO and partially the LUMO+1. Even so, the interpretation is not straightforward. For instance, the small energy difference (0.05 eV) between the LUMO+1 and LUMO+2 in the free PTCDA should be reflected in the STM images as a combination of both. Another additional question concerns the evolution of the five-stripe shape to a lobe shape for large positive voltages, this spatial distribution having no similarities with any of the calculated orbitals for the free molecule.

In order to clarify these issues and to get further insight into the bonding and charge-transfer mechanism, first-principles calculations of the interacting PTCDA/Si(111)-(7 \times 7) system have been performed. Norm-conserving pseudopotentials²⁹ are used in place of ionic core charges while a double- ζ plus polarization basis set represents the valence electrons. Total energies were computed with a 100 Ry plane-wave cutoff and using the Γ k point. Atomic forces were converged to better than 0.02 eV/Å. The silicon substrate was modeled using a repeated slab geometry with four layers of silicon; of these the lowest layer was kept fixed and saturated with hydrogen. Additionally, the PTCDA molecule was placed above the corner hole of the (7 \times 7) substrate in a planar configuration, according to the STM results. After geometry optimization of the system, it is found that PTCDA has a stable configuration on the corner hole site and that it binds through the corner oxygen atoms of the molecule to the four silicon adatoms belonging to adjacent unit cells [Fig. 1(d)]. The Si adatoms involved in the bonding suffer a subtle distortion in order to minimize the distance to the molecule. Structural relaxations

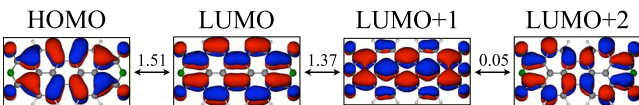


FIG. 2. (Color online) Wave functions $|\psi|^2$ for the HOMO, LUMO, LUMO+1, and LUMO+2 of a free PTCDA molecule in blue/red (dark gray/gray) according to sign(ψ). Their energy differences are shown above the arrows in electron volt.

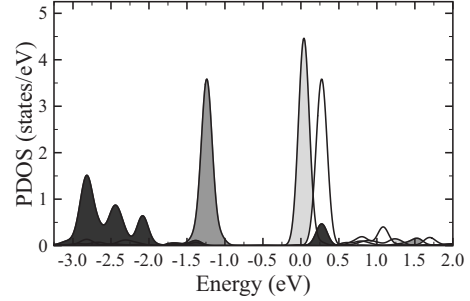


FIG. 3. PDOS of the PTCDA/Si(111)-(7 \times 7) system onto the HOMO (dark gray), LUMO (gray), LUMO+1 (light gray), and LUMO+2 (white), calculated for the isolated molecule in the adsorbed configuration, using a broadening of 0.1 eV.

are also found for PTCDA, these being mostly localized on the original C=O groups involved in the bonding (their bond length increases $\sim +7.5\%$). Small or minor changes are also seen for the surrounding C—C ($\sim +4.2\%$) and C—O ($\sim -1.7\%$) bonds.

Relevant information about the electronic structure is given by the projected density of states (PDOS) of the interacting PTCDA/Si(111) onto the MOs of the isolated molecule. The PDOS spectra (Fig. 3) show that the LUMO and LUMO+1, originally unoccupied, are significantly shifted below their original energy positions. The former is completely filled, whereas the latter crosses the Fermi level, being therefore partially filled. These results support the interpretation of the five-stripe pattern observed in STM images of occupied states as related to the unperturbed LUMO+1. The calculated spectra also present a rigid shift in energy mainly for occupied states. The energy differences between the MOs of the adsorbed molecule match well those corresponding to the free PTCDA. For positive energies, however, the energy difference between the LUMO+1 and LUMO+2 increases to $\sim 0.25 \text{ eV}$. Besides the mentioned shifts, considerable splittings of some of the MOs are observed in the spectra. In particular, the highest occupied molecular orbital (HOMO) contribution is evident in a wide energy range, between -3.0 and -2.0 eV , yet also unexpectedly present in unoccupied states, as a low but significant intensity peak around $+0.3 \text{ eV}$. The LUMO+2 components are found at $+0.3$ and $+1.0 \text{ eV}$.

Generally, large energy splittings may occur when the interacting orbitals belong to the same symmetry and when an efficient overlap exists between them. Hence, MOs undergoing splittings should interact with the substrate orbitals of matching symmetry and be localized around similar energy regions. Figure 4(a) displays the calculated DOS of silicon projected onto the atomic orbitals of the corner adatoms involved in the bonding. As it is well known, there exists a maximum near the Fermi energy related to the dangling-bond (DB) states of adatoms. Only two of these wave functions, corresponding to 0.0 and $+0.02 \text{ eV}$ [Figs. 4(b) and 4(c)], share the symmetry with that of the HOMO and LUMO+2 (Fig. 2). The existence of these silicon states with high DOS and identical symmetry as those MOs supports an efficient overlap, explaining thus the large splitting of the HOMO and LUMO+2, which ultimately leads to the appear-

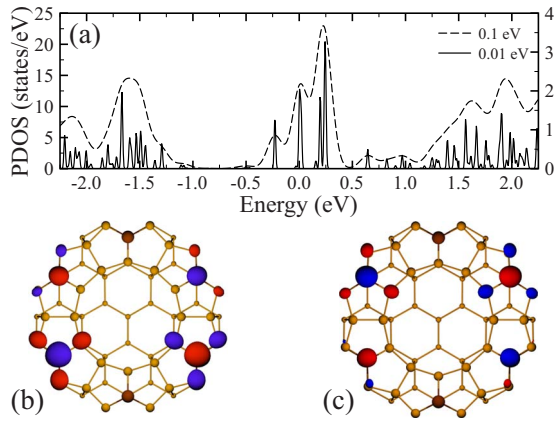


FIG. 4. (Color online) (a) PDOS of the Si(111) surface on the Si adatoms involved in the bonding, using broadenings of 0.1 and 0.01 eV. [(b) and (c)] Spatial charge distribution of the states localized at 0.0 eV and +0.02 eV, respectively. Blue/red colors stand for the sign of the wave function. The schematic view is centered on the corner hole of the silicon reconstruction.

ance of HOMO character just above the Fermi energy. Similarly, the HOMO becomes largely broadened near ~ -2.5 eV through interactions with the several symmetry-compatible states on the silicon adatoms in that energy region.

STM images were first simulated using the Tersoff and Hamann approximation³⁰ (see Fig. 5). While the image for the local density of states (LDOS) integrated from E_F to -1.0 eV fairly reproduces the five-stripe pattern observed in occupied states, the intramolecular features obtained in LDOS images integrated from E_F to $+0.5$ eV have neither the symmetry nor the shape resolved in the experimental STM images recorded at low positive voltage. This discrepancy motivated more involved calculations, including a realistic STM tip formed by ten Si atoms in a (111) pyramidal arrangement. Experimentally, atomic resolution in STM images was often obtained after intentional slight tip-sample contacts, which may lead to Si termination of the original W tips. More details can be found in Ref. 27.

A series of topographic STM images measured at different voltages are displayed in Fig. 6 (top) together with the

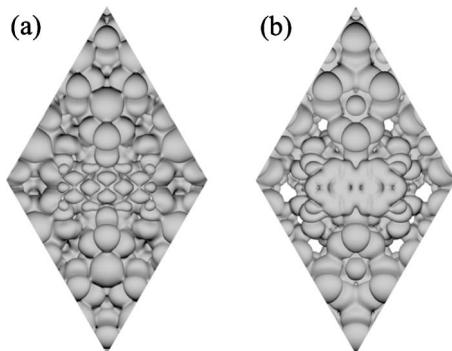


FIG. 5. Calculated STM images for occupied and unoccupied states in the Tersoff-Hamann approximation, i.e., the LDOS integrated from the Fermi level to (a) -1.0 eV and (b) $+0.5$ eV, respectively.

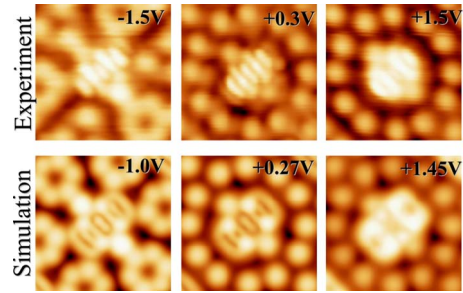


FIG. 6. (Color online) Comparison of experimental (top) and simulated (bottom) constant-current STM images of a PTCDA molecule adsorbed on Si(111)-(7 \times 7) for different bias voltages. Set point: 0.13 nA; images size: 3.2 \times 3.2 nm².

corresponding simulated ones (bottom). A fairly good agreement is found over a wide range of energies and tip-sample distances, where the simulations reproduce the shape, symmetry, and apparent size of single molecule features, both for unoccupied and occupied states. Thus, the theoretical image at a large positive bias ($+1.45$ V) reproduces well the intramolecular features resolved in the STM image, characterized by the oval-like shape separated by a depression. For voltages close to the Fermi energy, the simulated image reproduces the five parallel stripes pattern characteristic of experimental images. In the simulation at -1.0 V, the intramolecular features can also be described by several parallel stripes, reproducing the molecular shape resolved in the experimental STM image acquired at -1.5 V. This good agreement suggests that tip states represent an important factor to reproduce and interpret experimental images.

The complexity of the observed molecular features is itself interesting. In this kind of systems it is not very common to obtain such significant variations with respect to the MOs of the free molecule, particularly for energies close to E_F . A charge-transfer process from substrate to molecule usually results in partially filling of the LUMO, which would predominantly contribute to the tunneling current, up to large positive and negative biases. In our case, a series of competing factors, such as a strong charge transfer, positioning of LUMO+1 at E_F , almost degenerate LUMO+1 and LUMO+2, and the large splittings of orbitals, give rise to a non-trivial appearance of MOs in STM images, which is nevertheless reproduced by inclusion of realistic tips.

A final issue we have addressed is related to the bonding

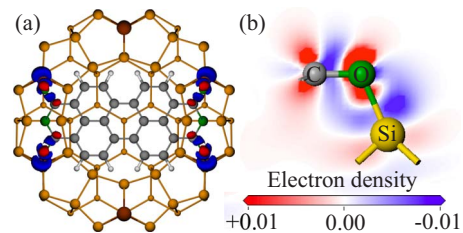


FIG. 7. (Color online) Electron density $\delta\rho$ in units of electrons/bohr³. (a) Top view of a PTCDA molecule upon the corner hole position at the Si(111)-(7 \times 7) surface. Isodensity surfaces at ± 0.01 are rendered in blue/red. (b) Color map for a plane crossing the Si—O—C bonds.

mechanism. The induced charge distribution $\delta\rho$ is visualized in Fig. 7(a), as the difference in electron density between the total system and the adsorbate and substrate. The plot shows a net negative charge localized mainly at the oxygen atoms involved in the bonding, and the absence of charge around the silicon atoms, thereby confirming the charge transfer from the partially occupied DBs into the oxygen atoms of the C=O groups. This is also evident from the color map of the Si—O—C plane shown in Fig. 7(b) and is consistent with the formation of a partially ionic covalent Si—O bond.

In summary we present a combined experimental STM and theoretical DFT study on the adsorption of a single

PTCDA molecule on the Si(111)-(7×7) substrate. The strong molecule-substrate coupling results in an intricate broadening, shift and splitting of MOs, contributing in a complex way to the tunnel current. Comprehensive electronic-structure calculations and detailed simulations of STM images turn out to be essential in understanding the interaction mechanisms existing at the interface of a complex molecule-semiconductor system.

Financial support from Spain's MEC under Grants No. MAT2007-60686, No. MAT2008-01497, and No. FIS2009-12712 and Comunidad de Madrid through Grant No. S2009/MAT-1467 and FPI program is gratefully acknowledged.

- ¹S. R. Forrest, *Chem. Rev.* **97**, 1793 (1997).
- ²J. I. Pascual, J. Gómez-Herrero, C. Rogero, A. M. Baró, D. Sánchez-Portal, E. Artacho, P. Ordejón, and J. M. Soler, *Chem. Phys. Lett.* **321**, 78 (2000).
- ³X. H. Lu, M. Grobis, K. H. Khoo, S. G. Louie, and M. F. Crommie, *Phys. Rev. Lett.* **90**, 096802 (2003).
- ⁴J. Repp, G. Meyer, S. M. Stojković, A. Gourdon, and C. Joachim, *Phys. Rev. Lett.* **94**, 026803 (2005).
- ⁵R. Temirov, S. Soubatch, A. Luican, and F. S. Tautz, *Nature (London)* **444**, 350 (2006).
- ⁶W.-H. Soe, C. Manzano, A. De Sarkar, N. Chandrasekhar, and C. Joachim, *Phys. Rev. Lett.* **102**, 176102 (2009).
- ⁷L. Gross, F. Mohn, N. Moll, P. Liljeroth, and G. Meyer, *Science* **325**, 1110 (2009).
- ⁸B. Xu and N. J. Tao, *Science* **301**, 1221 (2003).
- ⁹G. Schulze, K. J. Franke, A. Gagliardi, G. Romano, C. S. Lin, A. L. Rosa, T. A. Niehaus, Th. Frauenheim, A. Di Carlo, A. Pecchia, and J. I. Pascual, *Phys. Rev. Lett.* **100**, 136801 (2008).
- ¹⁰Y. F. Wang, J. Kröger, R. Berndt, H. Vázquez, M. Brandbyge, and M. Paulsson, *Phys. Rev. Lett.* **104**, 176802 (2010).
- ¹¹F. S. Tautz, *Prog. Surf. Sci.* **82**, 479 (2007).
- ¹²B. Uder, C. Ludwig, J. Petersen, B. Gompf, and W. Eisenmenger, *Z. Phys. B: Condens. Matter* **97**, 389 (1995); Q. Chen, T. Rada, T. Bitzer, and N. V. Richardson, *Surf. Sci.* **547**, 385 (2003); G. Sazaki, T. Fujino, J. T. Sadowski, N. Usami, T. Ujihara, K. Fujiwara, Y. Takahashi, E. Matsubara, T. Sakurai, and K. Nakajima, *J. Cryst. Growth* **262**, 196 (2004).
- ¹³Y. Hirose, S. R. Forrest, and A. Kahn, *Phys. Rev. B* **52**, 14040 (1995); D. A. Tenne, S. Park, T. U. Kampen, A. Das, R. Scholz, and D. R. T. Zahn, *ibid.* **61**, 14564 (2000); N. Nicoara, O. Custance, D. Granados, J. M. García, J. M. Gómez-Rodríguez, A. M. Baró, and J. Méndez, *J. Phys.: Condens. Matter* **15**, S2619 (2003).
- ¹⁴J. C. Swarbrick, J. Ma, J. A. Theobald, N. S. Oxtoby, J. N. O'Shea, N. R. Champness, and P. H. Beton, *J. Phys. Chem. B* **109**, 12167 (2005); J. B. Gustafsson, H. M. Zhang, and L. S. O. Johansson, *Phys. Rev. B* **75**, 155414 (2007); N. Nicoara, Z. Wei, and J. M. Gómez-Rodríguez, *J. Phys. Chem. C* **113**, 14935 (2009).
- ¹⁵R. A. Wolkow, *Annu. Rev. Phys. Chem.* **50**, 413 (1999).
- ¹⁶M. A. Filler and S. F. Bent, *Prog. Surf. Sci.* **73**, 1 (2003).
- ¹⁷F. Tao and G. Q. Xu, *Acc. Chem. Res.* **37**, 882 (2004).
- ¹⁸T. R. Leftwich and A. V. Teplyakov, *Surf. Sci. Rep.* **63**, 1 (2008).
- ¹⁹F. Tao, S. L. Bernasek, and G. Q. Xu, *Chem. Rev.* **109**, 3991 (2009).
- ²⁰A. Vilan, O. Yaffe, A. Biller, A. Salomon, A. Kahn, and D. Cahen, *Adv. Mater.* **22**, 140 (2010).
- ²¹E. Umbach, *Prog. Surf. Sci.* **35**, 113 (1990); M. Jung, U. Baston, G. Schnitzler, M. Kaiser, J. Papst, T. Porwol, H. J. Freund, and E. Umbach, *J. Mol. Struct.* **293**, 239 (1993); J. Taborski, P. Väterlein, H. Dietz, U. Zimmermann, and E. Umbach, *J. Electron Spectrosc. Relat. Phenom.* **75**, 129 (1995).
- ²²H. Vázquez, R. Oszwaldowski, P. Pou, J. Ortega, R. Pérez, F. Flores, and A. Kahn, *Europhys. Lett.* **65**, 802 (2004).
- ²³N. Nicoara, E. Román, J. M. Gómez-Rodríguez, J. A. Martín-Gago, and J. Méndez, *Org. Electron.* **7**, 287 (2006).
- ²⁴W. Kohn and L. J. Sham, *Phys. Rev.* **140**, A1133 (1965); J. P. Perdew and A. Zunger, *Phys. Rev. B* **23**, 5048 (1981).
- ²⁵P. Ordejón, E. Artacho, and J. M. Soler, *Phys. Rev. B* **53**, R10441 (1996).
- ²⁶J. M. Soler, E. Artacho, J. D. Gale, A. García, J. Junquera, P. Ordejón, and D. Sánchez-Portal, *J. Phys.: Condens. Matter* **14**, 2745 (2002).
- ²⁷O. Paz, I. Brihuega, J. M. Gómez-Rodríguez, and J. M. Soler, *Phys. Rev. Lett.* **94**, 056103 (2005); O. Paz and J. M. Soler, *Phys. Status Solidi B* **243**, 1080 (2006).
- ²⁸I. Horcas and R. Fernández, J. M. Gómez-Rodríguez, J. Colchero, J. Gómez-Herrero, and A. M. Baró, *Rev. Sci. Instrum.* **78**, 013705 (2007).
- ²⁹N. Troullier and J. L. Martins, *Phys. Rev. B* **43**, 1993 (1991).
- ³⁰J. Tersoff and D. R. Hamann, *Phys. Rev. B* **31**, 805 (1985).